Regenerative Therapy 26 (2024) 71–79

Contents lists available at ScienceDirect

Regenerative Therapy

journal homepage: http://www.elsevier.com/locate/reth

Original Article

Exploring SSEA3 as an emerging biomarker for assessing the regenerative potential of dental pulp-derived stem cells

Jumpei Shirakawa [a, *, 1], Edward H. Ntege [a, b, 1], Masuo Takemura [a], Sho Miyamoto [c], Toshihiro Kawano [a], Chisato Sampei [e], Hayato Kawabata [e], Hiroyuki Nakamura [a], Hiroshi Sunami [d], Tadayoshi Hayata [e], Yusuke Shimizu [b]

[a] Department of Oral and Maxillofacial Surgery, and Graduate School of Medicine, University of the Ryukyus, 207 Uehara, Nakagami, Nishihara, Okinawa 903-0215, Japan
[b] Department of Plastic and Reconstructive Surgery, Graduate School of Medicine, University of the Ryukyus, 207 Uehara, Nakagami, Nishihara, Okinawa 903-0215, Japan
[c] Department of Oral Surgery, Sapporo Medical University School of Medicine, South 1 West 16, Chuo-ku, Sapporo, Hokkaido, 060-8543, Japan
[d] Advanced Medical Research Center, Faculty of Medicine, University of the Ryukyus, 207 Uehara, Nishihara, Nakagami, Okinawa, 903-0215, Japan
[e] Department of Molecular Pharmacology, Graduate School of Pharmaceutical Sciences and Faculty of Pharmaceutical Science, Tokyo University of Science, 2641 Yamazaki, Noda, Chiba 287-8510, Japan

ARTICLE INFO

Article history:
Received 23 March 2024
Received in revised form
30 April 2024
Accepted 9 May 2024

Keywords:
Stage-specific embryonic antigen-3
Dental pulp
Stem cells
Regenerative medicine
Cellular senescence
Biomarker
Muse cell

ABSTRACT

Background: Human dental pulp-derived stem cells (hDPSCs) have emerged as a promising source for adult stem cell-based regenerative medicine. Stage-specific embryonic antigen 3 (SSEA3) is a cell surface marker associated with Multilineage-differentiating stress-enduring (Muse) cells, a subpopulation of human bone marrow-derived stem cells (hBMSCs), known for their potent regenerative potential and safety profile. In this study, we investigated the influence of the prolonged culture period and the number of culture passages on the regenerative capacity of hDPSCs and explored the association between SSEA3 expression and their regenerative abilities.

Methods: hDPSCs were isolated and cultured for up to 20 passages. Cell proliferation, migration, and osteogenic, adipogenic and neurogenic differentiation potential were assessed at passages 5, 10, and 20. Flow cytometry and immunofluorescence were employed to analyze SSEA3 expression. RNA sequencing (RNA-seq) was performed on SSEA3-positive and SSEA3-negative hDPSCs to identify differentially expressed genes and associated pathways.

Results: Our findings demonstrated a progressive decline in hDPSCs proliferation and migration capacity with increasing passage number. Conversely, cell size exhibited a positive correlation with passage number. Early passage hDPSCs displayed superior osteogenic and adipogenic differentiation potential. Notably, SSEA3 expression exhibited a significant negative correlation with passage numbers, reflecting the observed decline in differentiation capacity. RNA-seq analysis revealed distinct transcriptional profiles between SSEA3-positive and SSEA3-negative hDPSCs. SSEA3-positive cells displayed upregulation of genes associated with ectodermal differentiation and downregulation of genes involved in cell adhesion.

Conclusions: This study elucidates the impact of passaging on hDPSC behavior and suggests SSEA3 as a valuable biomarker for evaluating stemness and regenerative potential. SSEA3-positive hDPSCs,

Abbreviations: MTT, 3-(4,5-dimethylthiazol-2-yl)-2,5-diphenyltetrazolium bromide; ALP, alkaline phosphatase; BGLAP, gamma-carboxyglutamate protein; GAPDH, glyceraldehyde 3-phosphate dehydrogenase; hBMSCs, human bone marrow-derived stem cells; hDPSCs, Human dental pulp-derived stem cells; LPL, lipoprotein lipase; MSCs, mesenchymal stem cells; Muse cells, multilineage-differentiating stress-enduring cells; PAX6, paired box 6; PCDHB6, protocadherin Beta 6; PCDHG, protocadherin gamma subfamily; qPCR, quantitative real-time PCR; RT, reverse transcription; ARHGDIG, rho GDP dissociation inhibitor gamma; RNA-seq, RNA sequencing; SCHIP, schwannomin interacting protein; SOX2, SRY-box transcription factor 2; SSEA3, stage-specific embryonic antigen 3.

* Corresponding author. Department of Oral and Maxillofacial Surgery, Graduate School of Medicine, University of the Ryukyus, Nishihara, Okinawa 903-0215, Japan.
E-mail address: juneosur0610@gmail.com (J. Shirakawa).

Peer review under responsibility of the Japanese Society for Regenerative Medicine.

[1] These authors contributed equally to this work.

https://doi.org/10.1016/j.reth.2024.05.004

functionally analogous to Muse cells, represent a promising cell population for developing targeted regenerative therapies with potentially improved clinical outcomes.

1. Introduction

Adult mesenchymal stromal cells (MSCs) have emerged as a foundation of regenerative medicine due to their capacity for self-renewal, differentiation into diverse cell lineages, and promotion of tissue homeostasis and repair [1–3]. Derived from various sources such as bone marrow, adipose tissue, perinatal tissues, and dental pulp, MSCs offer a promising avenue for therapeutic interventions [3–6]. Human dental pulp stem cells (hDPSCs) have garnered significant interest as a readily available source of MSCs with substantial potential for clinical applications [7–10]. However, a critical knowledge gap remains regarding the impact of extended culture duration (passage number) on hDPSC differentiation potential in vitro [11–16].

Stage-Specific Embryonic Antigen 3 (SSEA3) is a cell surface glycosphingolipid belonging to the Lewis antigen family of carbohydrate antigens involved in crucial embryonic developmental processes, including cell adhesion, differentiation, and cell fate determination [17]. Its expression is associated with enhanced self-renewal capacity and pluripotency, suggesting a vital role in maintaining stem cell characteristics [18]. Studies have identified a subpopulation of human bone marrow-derived stem cells (hBMSCs) expressing SSEA3, termed Multilineage-differentiating stress-enduring (Muse) cells, which exhibit superior regenerative properties compared to conventional MSCs [19–22]. In contrast to conventional MSCs, which exert therapeutic effects primarily through these mechanisms, Muse cells offer distinct advantages such as non-surgical administration, spontaneous differentiation into tissue-specific cells to replace damaged cells, direct transplantation without the need for human leukocyte antigen (HLA)-matching or immunosuppression, long-lasting anti-inflammatory effects, and a low risk of tumorigenesis [19–27]. The expression pattern of SSEA3 in hDPSCs not only indicates their differentiation potential but also presents an opportunity to investigate their potential classification as dental pulp-derived Muse cells.

The present study aims to investigate the influence of culture duration on hDPSCs characteristics, including proliferation, migration, and differentiation potential, to gain a deeper understanding of their regenerative capacity. In the study, we propose that SSEA3 serves as a unique cell surface marker for monitoring differentiation potential over extended culture and may facilitate the identification of a subpopulation of hDPSCs-derived Muse cells with enhanced therapeutic potential. By elucidating the relationship between SSEA3 expression and hDPSCs behavior, this research can contribute significantly to advancing hDPSCs-based therapies for clinical use and pave the way for targeted regenerative treatments utilizing dental pulp-derived Muse cells.

2. Materials and methods

2.1. Isolation, culture, and differentiation of hDPSCs

2.1.1. Cell source and isolation

Impacted wisdom teeth were obtained from patients aged between 16 and 30 undergoing surgical procedures at Ryukyu University Hospital Dental and Oral Surgery with written informed consent (parental consent required for participants under 20) under a protocol approved by the University's Ethics Committee (approval no.: 1907). Exclusion criteria included individuals deemed unsuitable for participation by the attending dentist, those diagnosed with infectious diseases (Hepatitis B and C, Human immune deficiency virus (HIV), Human T-cell lymphotropic virus type 1 (HTLV-1), or syphilis), complications of diabetes, osteomyelitis, jaw bone cyst, or malignant tumor, and those with apical periodontitis, pulp gangrene, or pulpitis. Following tooth extraction under sterile conditions, teeth were transported in perfusion buffer (Perfusion Solution MOD. #1; Mediatech, Inc.) supplemented with 1% antibiotics (penicillin and streptomycin) on ice to the laboratory. After removing surrounding tissue, the teeth were vertically sectioned, and the dental pulp tissue was carefully dissected and chopped into small pieces. They were then incubated with digestive enzyme (Liberase; Roche) at 37 °C for 90 min with gentle shaking to isolate individual cells. (Fig. 1A–C).

2.1.2. Cell culture

The isolated cells were cultured in Lonza's human Adipose-Derived Stem Cell Growth BulletKit™ medium (ADSC-BM) for stem cell growth. The medium was changed every other day until the cells reached near confluency (80–90% coverage of the culture dish) (Fig. 1D). Primary cultured cells (passage 0, P0) were subsequently passaged to generate P1 cells. Then, subsequent passages were performed based on predetermined cell density criteria to maintain optimal growth. Cells at passages 5, 10, and 20 were cryopreserved for future experiments.

2.1.3. Differentiation induction

To induce differentiation into specific cell types, hDPSCs were cultured in lineage-specific conditioned media as previously reported [28]. Briefly, for neuronal differentiation, hDPSCs were cultured in serum-free human neural proliferation medium (StemCell Technologies, Canada) supplemented with epidermal growth factor (20 ng/ml) and basic fibroblast growth factor (10 ng/ml) as growth factors and 1% antibiotics at 37 °C in a 5% CO_2 atmosphere. For osteogenic differentiation, cells were cultured in α-MEM supplemented with 10% FBS, 1% antibiotics, 10 nM dexamethasone, 0.1 mM ascorbic acid-2-phosphate, and 10 mM β-glycerophosphate for the indicated culture period. Adipogenic differentiation was induced using DMEM supplemented with 10% FBS, 1% antibiotics, 100 nM dexamethasone, 0.25 mM indomethacin, 0.1 mM 3-isobutyl-1-methylxanthine, and 0.01 M insulin. Differentiation media were replaced every 3 days, and cells were maintained for 18 days. After differentiation protocols, cells were evaluated using specific staining procedures to confirm successful differentiation. Alizarin Red S staining was performed to visualize calcium deposition in osteogenic cultures, while Oil Red O staining by using kit (ScyTek Laboratories, Inc.) was used to identify lipid droplets within adipocytes.

2.2. Gene expression analysis

Total ribonucleic acid (RNA) was isolated from hDPSCs cultured under each condition using an RNA isolation kit (RNeasy Mini Kit;

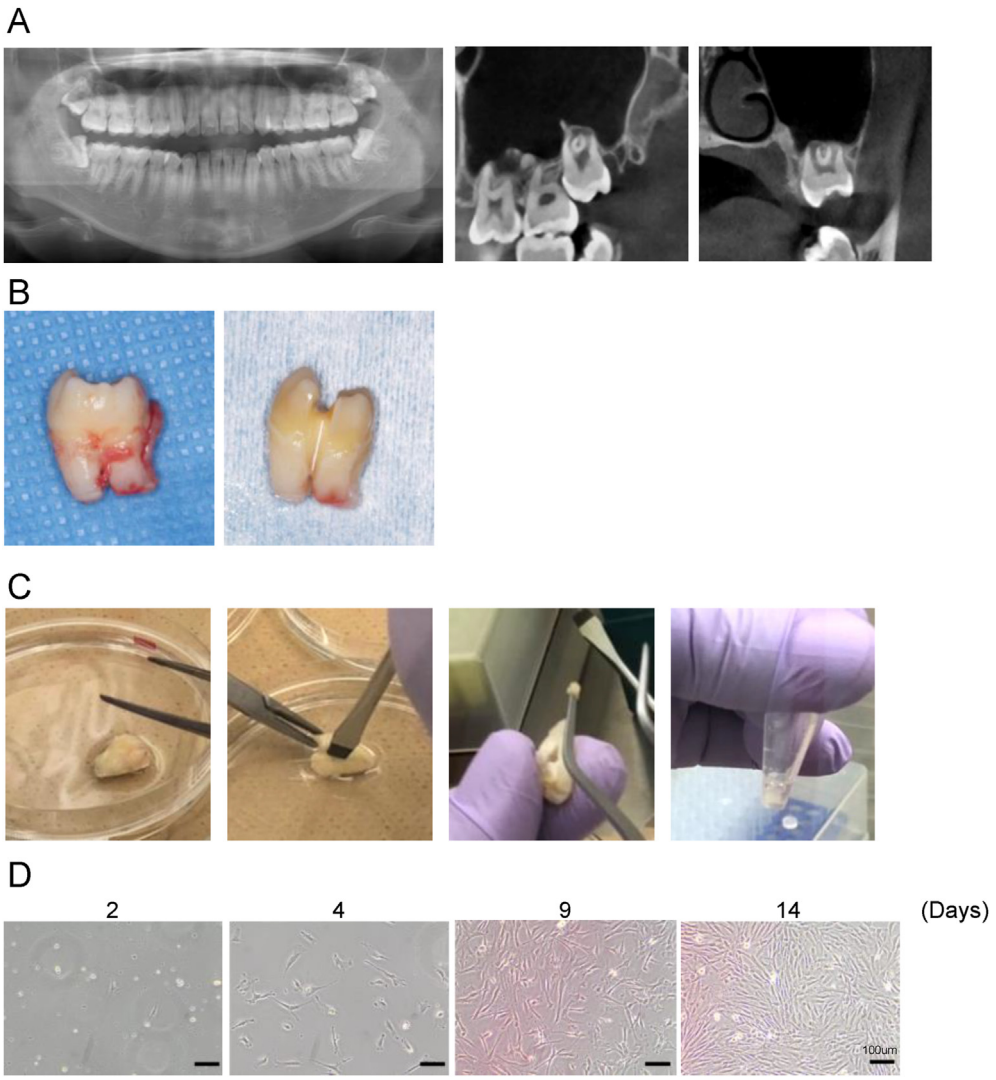

Fig. 1. hDPSC Isolation and Culture. (A) Panoramic radiograph and Sagittal and coronal plane image of corn beam computed tomography (CBCT) images of impacted wisdom teeth. (B) Extracted wisdom tooth with removed periodontal ligament, sectioned. (C) Dental pulp isolated for hDPSC isolation using enzyme digestion. (D) Primary hDPSCs reaching subconfluence after 10–14 days in culture.

Qiagen) according to the manufacturer's protocol. The quality and quantity of RNA were assessed using a NanoDrop. Reverse transcription (RT) was performed using 1 μg of total RNA and an RT-Polymerase Chain Reaction (PCR) solution (PrimerScript RT Master Mix; Takara) to obtain complementary deoxyribonucleic acid (cDNA). Quantitative real-time PCR (qPCR) was performed using a SYBR Green assay system (TB Green Premix Ex *Taq*II; TAKARA). The reagent mixture consists of 2 μL of the cDNA samples, 0.2 μM forward and reverse primers and 5 μL of PCR Master Mix for a total of 10 μL. The primer sequences for the targets are shown in Table 1. Each condition was analyzed at least three times. Glyceraldehyde 3-phosphate dehydrogenase (GAPDH) was used as the housekeeping gene. Cycle threshold (Ct) values for each gene were corrected using the mean Ct value. Gene expression levels were calculated using the ΔΔCt method, quantified using the $2^{-\Delta\Delta Ct}$ method, and normalized to the average Ct value for GAPDH gene expression levels.

2.3. Flow cytometry analysis and cell sorting

Each cultured cell was detached and extracted using a cell detachment solution, TrypLE™ Express (Gibco). A total of 5×10^5 cells per tube were incubated with 3 μL of fluorochrome-conjugated clusters of differentiation (CD) markers, including CD34, CD45, CD73, CD90, CD105, and CD133 (Biolegend), rat anti-human SSEA3 monoclonal antibody (MC631; Invitrogen), and rat Immunoglobulin M (IgM) (BioLegend) at 4 °C for 30 min. And the

Table 1
Primers and sequences for Real-time PCR analysis.

Primers	Sequences
GAPDH forward	5'-CAGGAGGCATTGCTGATGAT-3'
GAPDH reverse	5'-GAAGGCTGGGGCTCATTT-3'
SOX2 forward	5'-GTCACAGCATGATGCAGGACCA-3'
SOX2 reverse	5'-TCTGCGAGCTGGTCATGGAGTT-3'
ALP forward	5'-ACCATTCCCACGTCTTCACATTTG-3'
ALP reverse	5'-AGACATTCTCTCGTTCACCGCC-3'
BGLAP forward	5'-AGCCACCGAGACACCATGAGA-3'
BGLAP reverse	5'-GGCTGCACCTTTGCTGGACT-3'
LPL forward	5'-AGTAGCAGAGTCCGTGGCTA-3'
LPL reverse	5'-ATTCCTGTTACCGTCCAGCC-3'
NESTIN forward	5'-AACAGCGACGGAGGTCTCTA-3'
NESTIN reverse	5'-TTCTCTTGTCCCGCAGACTT-3'

GAPDH; human-specific glyceraldehyde 3-phosphate dehydrogenase, SOX2; SRY-box transcription factor 2, ALP; alkaline phosphatase, BGLAP; bone gamma-carboxyglutamate protein, LPL; Lipoprotein lipase (triacylglycerol acylhydrolase), NESTIN; neuroepithelial stem cell protein.

secondary antibody was FITC-conjugated anti-rat IgM (Jackson Immuno Research). Before analysis, stained cells were filtered through a 35 μm nylon filter into a conical tube and tagged with a blue dead cell stain (Invitrogen) to identify live and dead cells. FACS Verse (BD Biosciences) was used for flow cytometry analysis, and rat IgM was employed as a control. A flow cytometer (Sony SH800S Cell Sorter; Sony Biotechnology) and a perfusion buffer were used for cell sorting. According to the manufacturer's standards, a 130 μm sorting tip was used for cell sorting.

2.4. Cell proliferation assay

Cell viability of hDPSCs incubated for 48 h was assessed using the MTT assay according to the manufacturer's protocol (MTT Cell Proliferation Kit; Cayman Chemical Company). Briefly, cells (1×10^5/cm2) were seeded into 96-well plates and allowed to attach overnight; after 24 h of serum starvation, cells were cultured in standard culture media and then incubated with 20 μL of 3-(4,5-dimethylthiazol-2-yl)-2,5-diphenyltetrazolium bromide (MTT) solution (5 mg/mL) for 3 h. Colorimetric absorbance at 570 nm was measured using a microplate reader (iMark plate reader; BioRad).

2.5. Cell migration assay

A Boyden chamber insert (Culture-Insert 2 Well, Cat. No. 81176, ibidi) was employed to assess cell migration. Cells were seeded at a density of 1×10^5 cells per well and allowed to adhere overnight. Following incubation, the insert was carefully removed, creating a cell-free zone of 500 μm width. Fresh medium was then added to the wells. Images were captured at defined time points (0, 24, and 48 h) to monitor wound closure. ImageJ software (National Institutes of Health) was used to quantify the area of the wound at each time point. Wound closure was expressed as a percentage of the initial wound area at 0 h. Additionally, the average distance between the leading edges of the migrating cells was measured at 20 randomly chosen points per image.

2.6. Immunofluorescence staining of cultured DPSCs and dental pulp-derived Muse cells

Immunofluorescence staining was performed to assess the morphological features and quantify the SSEA3-positive cell population in hDPSCs. ImageJ, an image analysis software, was utilized to randomly measure the size of cultured hDPSCs from the captured images. A minimum of 20 cells were evaluated per image. To identify SSEA3, a rat-derived anti-SSEA3 antibody was used followed by incubation with goat anti-rat IgM conjugated with Alexa Fluor 647 (Jackson Immuno Research). Alexa Fluor 488 phalloidin (Cytoskeleton) was employed to visualize the actin cytoskeleton, and DAPI (8961S; Cell Signaling) was used for nuclear staining. Prolong Gold mounting medium was used to mount the stained samples.

2.7. RNA-seq analysis

Total RNA was extracted from SSEA3-positive or SSEA3-negative primary cultured hDPSCs using RNeasy Mini Kit (QIAGEN) according to the manufacturer's instructions. Poly-A + transcripts were purified using the NEBNext Ultra II Directional RNA Library Prep Kit for Illumina, and libraries were prepared using multiplexed barcode adaptors according to the manufacturer's instructions. High-throughput sequencing (150 bp, paired-end) was performed using the Illumina Novaseq 6000 with a sequencing depth of 40 million (20 million pairs) reads per sample. RNA-seq reads were tested for read quality after removing adapter sequences, and low-quality reads using Trimmomatic (version 0.39–1) and FastQC (version 0.12.0). First, HISAT2 (version 2.2.1) was used to map to the human genome obtained from GENCODE. Then, based on the mapping data, the expression levels of each gene were calculated using StringTie (version 2.2.1). Differentially expressed genes between samples were detected using the iDEGES/edgeR normalization method in the TCC package (FDR cut-off 10%). Genes with m.value > 1 and p.value < 0.05 were considered upregulated genes. Genes with m.value < 1 and p.value < 0.05 were considered downregulated genes. Gene enrichment analysis was performed using Metascape (version 3.5).

2.8. Statistical analysis

Data are presented as mean ± standard deviation (SD). Statistical analysis was performed using GraphPad Prism version 9.5.1(528) (San Diego, CA, USA). All data were tested for normality using the Shapiro-Wilk test. One-way analysis of variance (ANOVA) was followed by Tukey's multiple comparison test when comparing three or more groups with normally distributed data. The Kruskal-Wallis test with Dunn's multiple comparison test was used for data that did not follow a normal distribution. Error bars represent SD. P-values less than 0.05 were considered statistically significant. *p < 0.05, **p < 0.01, ***p < 0.001, ****p < 0.0001.

3. Results

3.1. Cell characteristics and differentiation potential of passaged hDPSCs

Since regenerative therapy requires a sufficient number of cells, sufficient cell proliferative capacity is essential. A cell proliferation experiments were performed after 48 h. The results showed no significant variation in passages 5 to 10. However, compared to the other two groups, cells at passage 20 decreased significantly (Fig. 2A). Interestingly, cell size increased with each successive passage. Cells at passage 20 were significantly larger than the other two groups, and the trend in cell size was similar to the trend in cell proliferation (Fig. 2B). Next, cell migration capacity was assessed on dedicated culture plates. After 24 h, cells at passage 5 exhibited a significant reduction in cell-free areas compared to the other two groups. They had completely covered the entire area in 48 h. In contrast, cells at passage 20 covered only approximately 50% of the area by 48 h. Cells at passage 10 showed a similar migration pattern at 24 h as those at passage 20, but by 48 h, they had reached the midpoint of the other two groups. Although the difference between cells at passage 10 and 5 was not statistically significant, their behavior significantly differed from those at passage 20 (Fig. 2C). These observations suggest that as the number of passages increases and cell size increases, the proliferative and migratory capacities of the cells decrease. Next, we examined the differentiation potential of hDPSCs into osteoblasts, adipocytes, and neurons by culturing them in a specific conditioned medium for 12 and 24 days. Expression of the pluripotency marker SRY-box transcription factor 2 (SOX2) showed a significant decrease with increasing number of passages and long-term cell culture (Fig. 2D). Expression of osteogenic differentiation markers alkaline Phosphatase (ALP) and bone gamma-carboxyglutamate protein (BGLAP) was increased in cells at passages 5 and 10, but not those at passage 20; there was a significant difference in BGLAP gene expression levels between passages 5 and 10, which was also confirmed by Alizarin red S staining (Fig. 2E). The adipogenic differentiation marker lipoprotein lipase (LPL) exhibited a similar trend of increased expression in cells at passages 5 and 10, but not those at passage 20. The Oil Red O

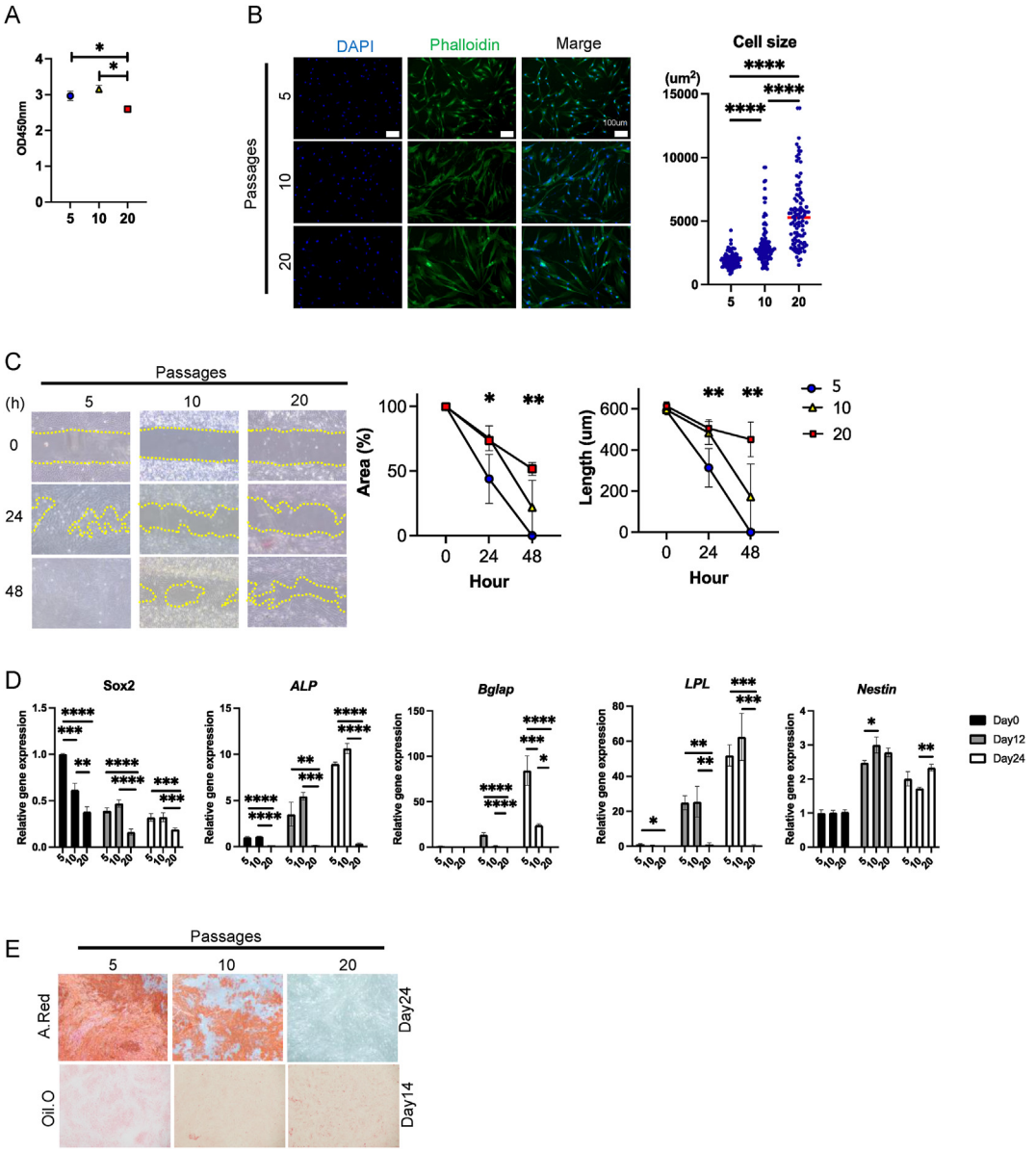

Fig. 2. Effects of Passage on hDPSC Characteristics. (A) Cell proliferation capacity was assessed using MTT assays after 48 h. Proliferation decreased at passage 20 compared to passages 5 and 10. (B) Left panel: representative immunostained images of hDPSCs. (Blue: DAPI, Green: Phalloidin) Scale bar: 100 μm. Cell size increased with passage number. (C) Left panel: representative cell migration assay images of each time points were exhibited. Migration capacity decreased with passage number. (D) Expression of pluripotency and osteogenic differentiation markers (Sox2 and Bglap) decreased with passage number. Expression of osteogenic and adipogenic differentiation markers (ALP and LPL) also decreased at passage 20 compared to passages 5 and 10, while Nestin, neural differentiation marker remained unchanged. (E) osteogenic and adipogenic differentiation (Alizarin Red and Oil Red O staining respectively) decreased with passage number.

staining was not very distinct but showed representative differences in the staining area between passages. Interestingly, Nestin, a marker of neural differentiation, increased significantly in all passaged cells during the initial time point in culture and remained stable after that but did not differ significantly by the number of passages. These findings suggest that passages, especially more than 10 passages, significantly affect the multidifferentiation potential of hDPSCs, except for neural differentiation.

3.2. SSEA3 is a novel stemness marker of culture-expanded hDPSCs

We examined the expression of MSC surface markers, including CD73, CD90, and CD105 as positive markers and CD34, CD45, and CD133 as negative markers in hDPSCs by conventional flow cytometry. We wished to determine whether these markers could effectively identify hDPSCs, as is commonly reported, and whether their expression was affected by the number of passages. We found that the expression levels of all positive and negative markers did not differ significantly with increasing numbers of passages, although there was greater variation among samples (Fig. 3A and B). These results indicate that the expression of MSC surface markers may not be a reliable indicator of the cell characteristics of hDPSCs, namely differentiation and stemness, following expansion. A previous study has reported that a small population of commercially available hDPSC cell lines expresses SSEA3, a specific surface marker for Muse cells found on bone marrow- and adipose tissue-derived stem cells.

Pluripotent stem cells are generally identified using SSEA3, SSEA4, and TRA-1-60 and negative staining for SSEA-1 [18,29,30]. Therefore, we analyzed SSEA3-positive cell populations in isolated

hDPSCs using flow cytometry analysis. The percentage of SSEA3-positive cells in hDPSCs at passage 5 and below was measured, and approximately 2%–3% of hDPSCs expressed SSEA3. These SSEA3-positive cells also exhibited differential expression of positive MSC markers and no expression of negative markers (data not shown). The effects of different passages on SSEA3 expression in hDPSCs was examined by flow cytometry. The results demonstrated that SSEA3 expression significantly decreased as passages increased, and hDPSCs almost completely lacked the SSEA3-positive cell population at passage 20 (Fig. 3C). These findings suggest that SSEA3-positive cell population may serve as a novel marker for assessing the stemness of hDPSCs grown in culture.

3.3. Cell characteristics of SSEA3-positive hDPSCs

Next, we examined whether SSEA3-positive cells could be isolated from hDPSCs and grown sustainably. Approximately 2% of the original hDPSC population of SSEA3-positive cells were effectively isolated and cultured, reaching 80%–90% confluency after 9 days (Supplemental Fig. 1). Subsequent analysis of the cell population using the same gating strategy revealed that more than 20% of the cells were SSEA3-positive expressing and more than 99% of the stem cell markers CD90 and CD105, (Fig. 4A). When SSEA3-positive and negative hDPSCs were resorted, both exhibited rapid proliferation. The SSEA3-positive cell population proliferated faster than the negative population, although the difference was insignificant (data not shown). Next, to assess the stability of the numbers of SSEA3-positive cells during proliferation, immunofluorescence staining was performed at early time points, followed

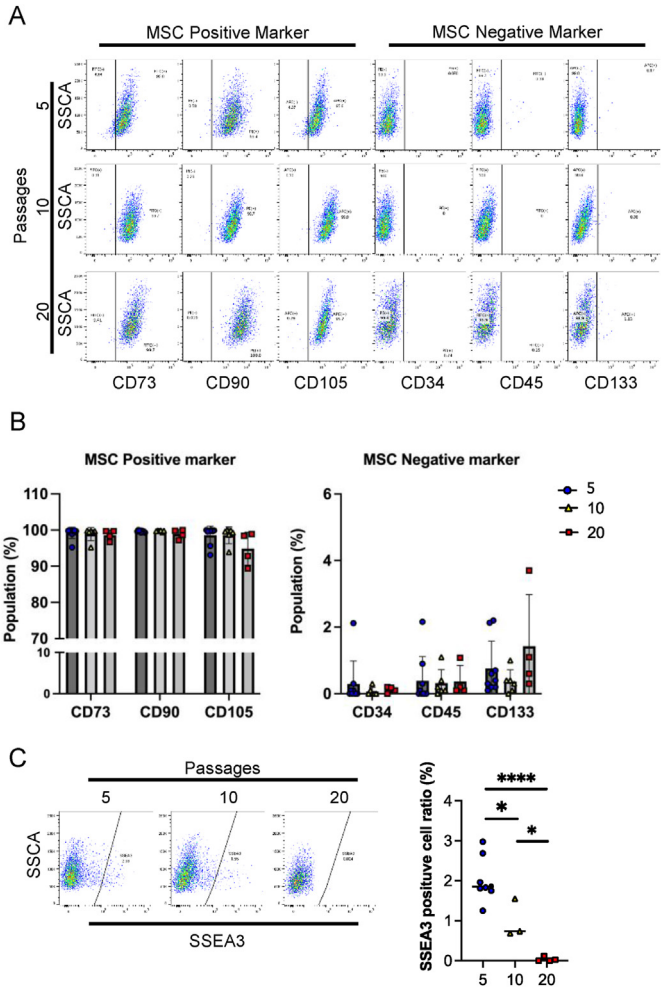

Fig. 3. Stem Cell Surface Markers and SSEA3 Expression in hDPSCs (A) Representative dot plots showing expression of stem cell markers (Positive: CD73, CD90 and Negative: CD105, CD34, CD45, CD133). (B) Bar graphs showing the positive cell population for each surface markers. No significant difference observed in each markers across passages. (C) Left panel: representative dot plots showing expression of SSEA3 in hDPSCs. SSEA3-positive cell population decreased with passage number.

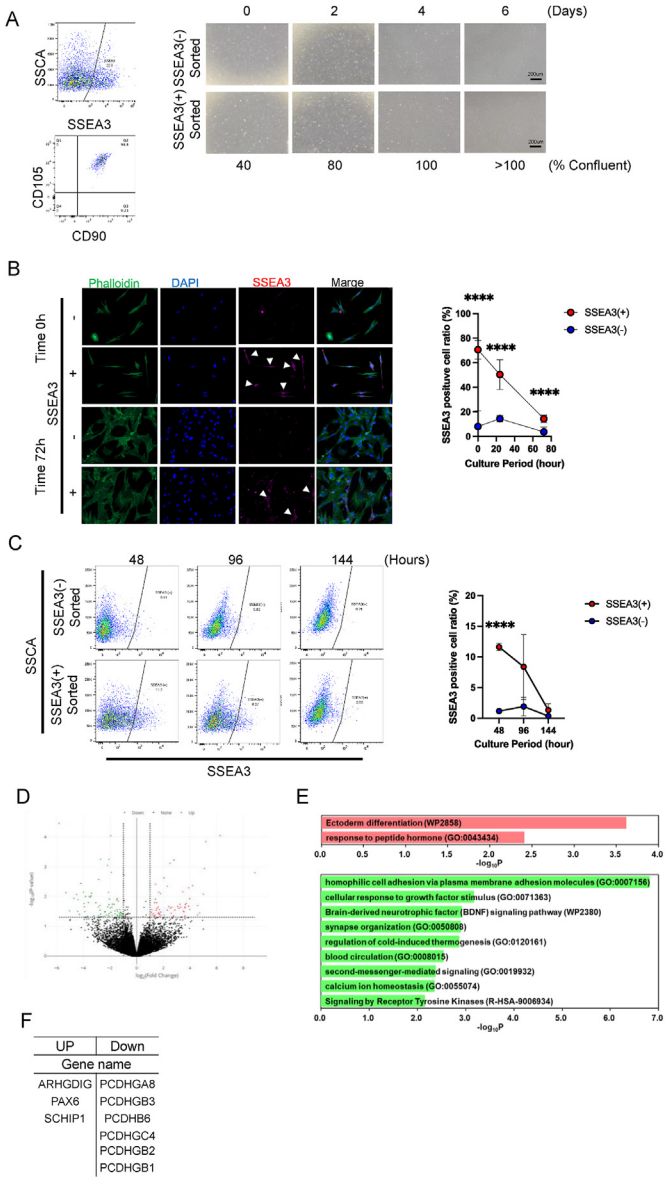

Fig. 4. Characteristics of SSEA3 positive hDPSCs. (A) Left panel: representative dot plots of SSEA3-positive cells in sorted hDPSCs and expression of CD90 and CD105 in resorted SSEA3-positive hDPSCs. Right panel: representative images of resorted SSEA3-positive and SSEA3-negative hDPSCs in culture. (B) Left panel: representative immunofluorescence staining images of resorted SSEA3-positive or negative hDPSCs using anti-SSEA3 antibody (red), phalloidin (green), and DAPI (blue). Arrowheads indicate SSEA3-positive cells. Decrease in SSEA3-positive cell population observed over culture period. (C) Left panel: representative dot plots of resorted SSEA3-positive or SSEA3-negative hDPSCs at each time point. Decrease in SSEA3-positive cell population observed in both resorted populations over culture period, with no significant difference after 96 h. (D) Volcano plot depicting differentially expressed genes in SSEA3-positive hDPSCs compared with SSEA3-negative. (green: upregulated, red: downregulated) (E) Metascape enrichment analysis identified pathways associated with up/downregulated genes in SSEA3-positive hDPSCs. (F) Specific genes showing altered expression in pathways identified by Metascape.

Table 2
Genes significantly up- or downregulated in SSEA3-positive hDPSCs identified by RNA-seq analysis.

Up regulated genes in DPSC derived SSEA3-positive cell			
Rank	Gene name	Rank	Gene name
1	RAB4B-EGLN2	16	PTGES3L-AARSD1
2	ABHD14A-ACY1	17	ELAVL2
3	RPS10-NUDT3	18	GPRC5D-AS1
4	MEF2B	19	GNRHR
5	SOGA3	20	ZNF763
6	SCHI P1	21	RN7SL130P
7	ABHD17AP4	22	RPS4XP16
8	UPK3BL1	23	ENO1-AS1
9	PAX6	24	ZNF887P
10	ADAM21P1	25	STX16-NPEPL1
11	LINC00167	26	LINC00663
12	PDCD6IPP1	27	ARHGDIG
13	AD000864.2	28	HMGA1P2
14	SNURF	29	TNFRSF11A
15	HEATR4	30	SLC16A14
Down regulated genes in DPSC derived SSEA3-positive cell.			
Rank	Gene name	Rank	Gene name
1	KRT8P47	25	TEN1
2	CBWD4P	26	NPIPB10P
3	PCDHGB2	27	IL18R1
4	ABCA8	28	MAPT
5	PCDHGB1	29	GALNT3
6	GRAP	30	SHC2
7	DUSP4	31	TACR2
8	GOLGA8M	32	FAM20A
9	LINC00545	33	FGF7P3
10	LINC01618	34	SPON2
11	LINC01013	35	POSTN
12	ENO1P1	36	PCDHGA8
13	ZNF608	37	PTGIS
14	GPR84	38	GPRC5C
15	TMTC1	39	MYH16
16	ACTL8	40	IMPG1
17	PALM	41	KSR2
18	CCL20	42	AQP7P1
19	FMOD	43	ALPL
20	PDE3A	44	SYNE1-AS1
21	ARL2-SNX15	45	PCDHGB3
22	TMEM178A	46	KCNN3
23	MYL4	47	PCDHGC4
24	PCDHB6		

by flow cytometry at later time points. Interestingly, almost all cells were attached 12 h after seeding, but the percentage of SSEA3-positive cells was about 80% (Fig. 4B). At 24 h, SSEA3-positive cells decreased by approximately 50%, and by 72 h, they represented about 20% of the population, as determined by immunofluorescence staining. The decrease in SSEA3-positive cells continued at later time points, and even after reaching confluency, less than 1% remained at 144 h (Fig. 4C). These findings indicate that the SSEA3-positive cell populations gradually decrease during proliferation, even after the cell population reaches confluency. This may support the use of SSEA3 as a valuable marker for assessing the regenerative potential of hDPSCs grown in culture.

3.4. Transcriptome analysis of SSEA3-positive hDPSCs

We performed RNA-seq to investigate gene expression of SSEA3-positive hDPSCs. The volcano plot indicates genes upregulated or downregulated in SSEA3-positive hDPSCs compared to SSEA3-negative hDPSCs (Fig. 4D). There were 30 upregulated and 47 downregulated genes in SSEA3-positive hDPSCs (Table 2). Gene enrichment analysis showed that the upregulated genes were enriched in gene ontology (GO) terms associated with “Ectoderm differentiation”, and the downregulated genes were enriched in that associated with “Homophilic cell adhesion via plasma membrane adhesion” molecule (Fig. 4 E). The ectoderm differentiation category includes Rho GDP Dissociation Inhibitor Gamma (ARHGDIG), Paired box (PAX) 6, and schwannomin interacting protein (SCHIP) genes. The homophilic cell adhesion via plasma membrane adhesion molecule includes Protocadherin Gamma Subfamily (PCDHG) A8, PCDHGB1, PCDHGB2, PCDHGB3, PCDHGC4, and Protocadherin Beta (PCDHB) 6 (Fig. 4 F).

4. Discussion

The in vitro differentiation potential of hDPSCs after extended culture expansion remains poorly defined [13–16]. This study aimed to explore the impact of passage number, a marker of culture expansion, on the characteristics of hDPSCs. Our results suggest that prolonged culturing significantly modifies hDPSC properties, potentially compromising their therapeutic efficacy in regenerative applications.

Cell proliferation assays revealed a decline in proliferation rate with increasing passage number. Interestingly, cell size also increased with passage number, suggesting a possible association between changes in cell morphology and decreased proliferation.

Further investigation is needed to determine if this increase in size is associated with cellular senescence, a state of replicative arrest. hDPSC migration capacity also exhibited a significant decrease with increasing passage number. This finding aligns with previous observations on other cell types in extended culture [14]. The pluripotency marker SOX2 displayed a gradual decrease in expression with increasing passage number, suggesting a potential loss of pluripotency and a shift towards a more lineage-restricted phenotype. We further explored the differentiation potential of hDPSCs at different passage numbers, focusing on osteogenesis, adipogenesis, and neurogenesis. Cells at early passages (5 and 10) exhibited greater osteogenic and adipogenic potential compared to those at later passages (passage 20). Remarkably, the neurogenic marker Nestin showed no significant difference by passage number, suggesting that the dental pulp's inherent neural crest origin may influence this specific lineage commitment. Whereas both SOX2 and SSEA3 expression decreased with increasing passage number, SSEA3 offers several advantages as a biomarker for evaluating the regenerative potential of hDPSCs. As a cell surface marker, SSEA3 allows for easier detection using flow cytometry without fixation or permeabilization, making it a more convenient tool for assessing live cell populations. Furthermore, SSEA3 is specifically associated with Muse cells, a subpopulation of mesenchymal stem cells known for their superior regenerative potential and non-tumorigenic properties [19–22]. Identifying and isolating this subpopulation using SSEA3 could lead to more targeted and effective cell-based therapies. Our study demonstrates that SSEA3 expression changes in parallel with the pluripotency and regenerative potential of hDPSCs, suggesting it may be a more reliable indicator of the cells' differentiation capacity over time compared to SOX2.

Despite the advancements presented here, some limitations necessitate consideration. The study employed specific passage numbers (5, 10, and 20) to investigate the effects of passaging on hDPSCs. While informative, these may not capture the full spectrum of changes throughout an extended culture period. Including additional intermediate passage numbers could provide a more complete picture of the sequential changes in hDPSC characteristics. The inherent challenges of in vitro cell culture models must also be acknowledged. The in vitro environment does not fully replicate the complex in vivo environment where hDPSCs reside. Therefore, caution is necessary when translating these findings to potential therapeutic applications. Future studies should incorporate in vivo functional assays using appropriate animal models to assess the true regenerative potential of hDPSCs.

Our study focused on SSEA3 as a potential biomarker for hDPSC stemness. However, other stage-specific embryonic antigens like SSEA1 and SSEA4 have also been implicated in stemness regulation [31,32]. Investigating the expression patterns of the entire SSEA family and their correlation with hDPSC regenerative potential could provide a more comprehensive understanding. Additionally, exploring the co-expression of SSEAs with other mesenchymal stem cell markers might help identify subpopulations with enhanced regenerative capabilities. RNA-seq analysis revealed specific gene expression changes associated with the SSEA3-positive hDPSC population. Future studies should validate the functional importance of these genes and their associated pathways in hDPSC-derived Muse cells. Employing single-cell RNA sequencing could offer further insights into the heterogeneity of the hDPSC population and potentially uncover subpopulations with unique characteristics and behaviors. Furthermore, maintaining low expression levels of genes associated with reduced regenerative capacity in SSEA3-positive cells may improve the overall yield of Muse cells during proliferation.

5. Conclusion

In summary, this study demonstrates that extended culture significantly alters hDPSC characteristics and potentially reduces their regenerative potential. SSEA3 emerged as a promising novel biomarker with a strong correlation to differentiation capacity. SSEA3-positive hDPSCs, representing the Muse cell population, possess a unique gene expression profile and hold great promise for targeted regenerative therapies.

Further research is crucial to fully elucidate the functional properties of SSEA3-positive hDPSCs. This includes validating their therapeutic efficacy in vivo through appropriate animal models. Additionally, optimizing isolation and expansion strategies for SSEA3-positive hDPSCs will be essential for their clinical application. Deciphering the co-expression of SSEA3 with other stem cell markers and its role in governing hDPSC fate and function will be critical for harnessing their full regenerative potential.

Author contributions

J.S conception and design, collection and/or assembly of data, data analysis and interpretation, manuscript writing.

E.H.N collection and/or assembly of data, data analysis, and interpretation, manuscript writing.

M.T collection and/or assembly of data, data analysis, and interpretation.

S.M collection and/or assembly of data.

T.K collection and/or assembly of data.

H.N provision of study material or patients.

H.S provision of study material or patients, data analysis, and interpretation.

Y.S financial support, data analysis, and interpretation.

C.S data analysis.

H.K data analysis.

T.H data analysis, interpretation, manuscript writing.

Funding

This work was supported by a grant from the Okinawa prefectural government through the Okinawa Innovation Ecosystem Joint Research Promotion Project (Grant ID not available).

Data availability statement

The datasets generated and/or analyzed during the current study are available from the corresponding author upon reasonable request.

Declaration of competing interest

The authors declare that they have no known competing financial interests or personal relationships that could have appeared to influence the work reported in this paper.

Acknowledgments

We thank Dr. Taro Ikegami, Assistant Professor, School of Medicine, Department of Otolaryngology and Neck Surgery, University of the Ryukyus, for his helpful suggestions and technical assistance. We also thank Enago (www.enago.jp) for assisting with language editing.

Appendix A. Supplementary data

Supplementary data to this article can be found online at https://doi.org/10.1016/j.reth.2024.05.004.

References

[1] Hoang DM, Pham PT, Bach TQ, Ngo ATL, Nguyen QT, Phan TTK, et al. Stem cell-based therapy for human diseases. Signal Transduct Targeted Ther 2022 Aug 6;7(1):272. https://doi.org/10.1038/s41392-022-01134-4.

[2] Pittenger MF, Mackay AM, Beck SC, Jaiswal RK, Douglas R, Mosca JD, et al. Multilineage potential of adult human mesenchymal stem cells. Science 1999 Apr 2;284(5411):143–7. https://doi.org/10.1126/science.284.5411.143.

[3] Ntege EH, Sunami H, Shimizu Y. Advances in regenerative therapy: a review of the literature and future directions. Regen Ther 2020 Feb 20;14:136–53. https://doi.org/10.1016/j.reth.2020.01.004.

[4] Shimizu Y, Ntege EH, Sunami H. Adipose tissue-derived regenerative cell-based therapies: current optimisation strategies for effective treatment in aesthetic surgery. InHandbook of Stem Cell Therapy 2022 Jun;22:1–33. https://doi.org/10.1007/978-981-16-6016-0_35-1. Singapore: Springer Nature Singapore.

[5] Barzegar M, Vital S, Stokes KY, Wang Y, Yun JW, White LA, et al. Human placenta mesenchymal stem cell protection in ischemic stroke is angiotensin converting enzyme-2 and masR receptor-dependent. Stem Cell 2021 Oct;39(10):1335–48. https://doi.org/10.1002/stem.3426.

[6] Roshandel E, Mehravar M, Dehghani Ghorbi M, Tabarraee M, Salimi M, Hajifathali A. Potential and challenges of placenta-derived decidua stromal cell therapy in inflammation-associated disorders. Hum Immunol 2022 Jul;83(7):580–8. https://doi.org/10.1016/j.humimm.2022.04.011.

[7] Siddiqui Z, Acevedo-Jake AM, Griffith A, Kadincesme N, Dabek K, Hindi D, et al. Cells and material-based strategies for regenerative endodontics. Bioact Mater 2021 Nov 30;14:234–49. https://doi.org/10.1016/j.bioactmat.2021.11.015.

[8] Lee YC, Chan YH, Hsieh SC, Lew WZ, Feng SW. Comparing the osteogenic potentials and bone regeneration capacities of bone marrow and dental pulp mesenchymal stem cells in a rabbit calvarial bone defect model. Int J Mol Sci 2019 Oct 10;20(20):5015. https://doi.org/10.3390/ijms20205015.

[9] Lew WZ, Feng SW, Lin CT, Huang HM. Use of 0.4-Tesla static magnetic field to promote reparative dentine formation of dental pulp stem cells through activation of p38 MAPK signalling pathway. Int Endod J 2019 Jan;52(1):28–43. https://doi.org/10.1111/iej.12962.

[10] Bu NU, Lee HS, Lee BN, Hwang YC, Kim SY, Chang SW, et al. In vitro characterization of dental pulp stem cells cultured in two microsphere-forming culture plates. J Clin Med 2020 Jan 16;9(1):242. https://doi.org/10.3390/jcm9010242.

[11] Dunn CM, Kameishi S, Grainger DW, Okano T. Strategies to address mesenchymal stem/stromal cell heterogeneity in immunomodulatory profiles to improve cell-based therapies. Acta Biomater 2021 Oct 1;133:114–25. https://doi.org/10.1016/j.actbio.2021.03.069.

[12] Luby AO, Ranganathan K, Lynn JV, Nelson NS, Donneys A, Buchman SR. Stem cells for bone regeneration: current state and future directions. J Craniofac Surg 2019 May/Jun;30(3):730–5. https://doi.org/10.1097/SCS.0000000000005250.

[13] Dou W, Xie J, Chen J, Zhou J, Xu Z, Wang Z, et al. Overexpression of adrenomedullin (ADM) alleviates the senescence of human dental pulp stem cells by regulating the miR-152/CCNA2 pathway. Cell Cycle 2023 Mar;22(5):565–79. https://doi.org/10.1080/15384101.2022.2135621.

[14] Morsczeck C. Cellular senescence in dental pulp stem cells. Arch Oral Biol 2019 Mar;99:150–5. https://doi.org/10.1016/j.archoralbio.2019.01.012.

[15] Rodier F, Campisi J. Four faces of cellular senescence. J Cell Biol 2011 Feb 21;192(4):547–56. https://doi.org/10.1083/jcb.201009094.

[16] Yi Q, Liu O, Yan F, Lin X, Diao S, Wang L, et al. Analysis of senescence-related differentiation potentials and gene expression profiles in human dental pulp stem cells. Cells Tissues Organs 2017;203(1):1–11. https://doi.org/10.1159/000448026.

[17] Suzuki Y, Haraguchi N, Takahashi H, Uemura M, Nishimura J, Hata T, et al. SSEA-3 as a novel amplifying cancer cell surface marker in colorectal cancers. Int J Oncol 2013 Jan;42(1):161–7. https://doi.org/10.3892/ijo.2012.1713.

[18] Draper JS, Smith K, Gokhale P, Moore HD, Maltby E, Johnson J, et al. Recurrent gain of chromosomes 17q and 12 in cultured human embryonic stem cells. Nat Biotechnol 2004 Jan;22(1):53–4. https://doi.org/10.1038/nbt922.

[19] Kuroda Y, Wakao S, Kitada M, Murakami T, Nojima M, Dezawa M. Isolation, culture and evaluation of multilineage-differentiating stress-enduring (Muse) cells. Nat Protoc 2013;8(7):1391–415. https://doi.org/10.1038/nprot.2013.076.

[20] Kuroda Y, Kitada M, Wakao S, Nishikawa K, Tanimura Y, Makinoshima H, et al. Unique multipotent cells in adult human mesenchymal cell populations. Proc Natl Acad Sci U S A 2010 May 11;107(19):8639–43. https://doi.org/10.1073/pnas.0911647107.

[21] Kushida Y, Wakao S, Dezawa M. Muse cells are endogenous reparative stem cells. Adv Exp Med Biol 2018;1103:43–68. https://doi.org/10.1007/978-4-431-56847-6_3.

[22] Noda T, Nishigaki K, Minatoguchi S. Safety and efficacy of human muse cell-based product for acute myocardial infarction in a first-in-human trial. Circ J 2020 Jun 25;84(7):1189–92. https://doi.org/10.1253/circj.CJ-20-0307.

[23] Fu Y, Karbaat L, Wu L, Leijten J, Both SK, Karperien M. Trophic effects of mesenchymal stem cells in tissue regeneration. Tissue Eng Part B 2017 Dec;23(6):515–28. https://doi.org/10.1089/ten.TEB.2016.0365.

[24] Alessio N, Squillaro T, Özcan S, Di Bernardo G, Venditti M, Melone M, et al. Stress and stem cells: adult Muse cells tolerate extensive genotoxic stimuli better than mesenchymal stromal cells. Oncotarget 2018 Apr 10;9(27):19328–41. https://doi.org/10.18632/oncotarget.25039.

[25] Fujita Y, Komatsu M, Lee SE, Kushida Y, Nakayama-Nishimura C, Matsumura W, et al. Intravenous injection of muse cells as a potential therapeutic approach for epidermolysis bullosa. J Invest Dermatol 2021 Jan;141(1):198–202.e6. https://doi.org/10.1016/j.jid.2020.05.092.

[26] Kuroda Y, Oguma Y, Hall K, Dezawa M. Endogenous reparative pluripotent Muse cells with a unique immune privilege system: Hint at a new strategy for controlling acute and chronic inflammation. Front Pharmacol 2022 Oct 19;13:1027961. https://doi.org/10.3389/fphar.2022.1027961.

[27] Yamada Y, Wakao S, Kushida Y, Minatoguchi S, Mikami A, Higashi K, et al. S1P-S1PR2 axis mediates homing of muse cells into damaged heart for long-lasting tissue repair and functional recovery after acute myocardial infarction. Circ Res 2018 Apr 13;122(8):1069–83. https://doi.org/10.1161/CIRCRESAHA.117.311648.

[28] Luke AM, Patnaik R, Kuriadom S, Abu-Fanas S, Mathew S, Shetty KP. Human dental pulp stem cells differentiation to neural cells, osteocytes and adipocytes-An in vitro study. Heliyon 2020 Jan 6;6(1):e03054. https://doi.org/10.1016/j.heliyon.2019.e03054. Erratum in: Heliyon. 2020 Feb 12;6(2):e03308.

[29] Draper JS, Pigott C, Thomson JA, Andrews PW. Surface antigens of human embryonic stem cells: changes upon differentiation in culture. J Anat 2002 Mar;200(3):249–58. https://doi.org/10.1046/j.1469-7580.2002.00030.x.

[30] Enver T, Soneji S, Joshi C, Brown J, Iborra F, Orntoft T, et al. Cellular differentiation hierarchies in normal and culture-adapted human embryonic stem cells. Hum Mol Genet 2005 Nov 1;14(21):3129–40. https://doi.org/10.1093/hmg/ddi345.

[31] Inada E, Saitoh I, Kubota N, Iwase Y, Murakami T, Sawami T, et al. Increased expression of cell surface SSEA-1 is closely associated with naïve-like conversion from human deciduous teeth dental pulp cells-derived iPS cells. Int J Mol Sci 2019 Apr 3;20(7):1651. https://doi.org/10.3390/ijms20071651.

[32] Kawanabe N, Murata S, Fukushima H, Ishihara Y, Yanagita T, Yanagita E, et al. Stage-specific embryonic antigen-4 identifies human dental pulp stem cells. Exp Cell Res 2012 Mar 10;318(5):453–63. https://doi.org/10.1016/j.yexcr.2012.01.008.